

# Influence of Spike Defect on the Impulse Breakdown Characteristics of SF<sub>6</sub> Gas Gap in GIS

Xuandong Liu, Lingli Zhang, Tao Wen and Qiaogen Zhang

State Key Laboratory of Electrical Insulation and Power Equipment,  
School of Electrical Engineering, Xi'an Jiaotong University,  
Xi'an, 710049, PR China

## ABSTRACT

By using 1 MV Marx generator and a 220 kV GIS bus, an experiment platform has been established, and a stainless steel needle is applied to simulate spike defect, so as to study the influence of pressure, wave front time and electric field on 50 % breakdown voltage ( $U_{50}$ ) and voltage-time ( $V-t$ ) characteristics of SF<sub>6</sub> gas gap with existence of a spike defect on the bus of GIS under double exponential impulse voltage. When wave front time is short, 50% breakdown voltage of the SF<sub>6</sub> gap hardly changes with various pressures, and  $U_{50}\text{-}P$  curve turns to be a hump shape when wave front time increases. However, pressure has no significant effect on  $V-t$  characteristics. The slope of  $V-t$  characteristics curve is negative when wave front time of applied voltage is short (0.08~0.9 $\mu$ s), and it will turn to be positive when wave front time becomes longer (several ~15 $\mu$ s). A new method to fit these  $V-t$  characteristics curves under impulse voltage with longer wave front times is proposed. It is found that 50 % breakdown voltage decreases almost linearly with the increase of electric field non-uniformity factors ( $f$ ), and  $V-t$  characteristics cluster with valley-like profile have been drawn at different  $f$ . Dispersion of  $V-t$  characteristics cluster reduces and the flat region expands with the increase of  $f$ , and minimum value of breakdown voltage of SF<sub>6</sub> gap with spike defect under impulse voltage, which is of guiding significance for engineering, can be obtained.

Index Terms — gas-insulated metal-enclosed switchgear, spike defect, 50% breakdown voltage, voltage-time characteristics, space charges

## 1 INTRODUCTION

DUE to high dielectric strength and ideal physicochemical properties, SF<sub>6</sub> is the most important medium for insulating and arc extinguishing in GIS (gas-insulated metal-enclosed switchgear) [1-4]. It is revealed by some researchers that SF<sub>6</sub> is quite sensitive to electric field non-uniformity factors  $f$  which means that once local electric field is too high to exceed certain value compared with average electric field strength in a SF<sub>6</sub> gas gap or along insulator surface, the insulation performance of SF<sub>6</sub> declines dramatically [5,6].

Taking tiny linear metal particles as an example, if this kind of particle exists on the bus of GIS, the distortion of local electric field may cause the reduction of partial discharge inception voltage and breakdown voltage, especially under lightning impulse (LI). As a consequence, GIS with various rated voltage levels are usually designed to be slightly non-uniform electric field. However, conductive particles in shape of linear, spherical, sheet, *etc.* may be formed in processes of

manufacture, transportation, assembly and operation. Although kinds of methods are applied in these processes, they cannot eliminate the influence of metal particles thoroughly. Therefore, high voltage tests such as power-frequency withstand voltage test, partial discharge test and impulse voltage test are applied to detect the underlying insulation defects and ensure the safe operation of GIS. Compared to the former two kinds of tests, impulse voltage test is extremely sensitive to abnormal electric field concentration in GIS [7, 8].

In recent years, numbers of researches on breakdown characteristics of SF<sub>6</sub> gas gap under impulse voltage were carried out in and abroad [9-14]. Zhifeng Guo studied the breakdown voltages of a 2 mm SF<sub>6</sub> gap with needle-plane electrodes in various gas pressures under oscillating impulse voltage with wave front time equivalent to lightning impulse, and an overall upward trend of breakdown voltages with the increase of gas pressure was found [12]. The influence of wave front time on breakdown characteristics of a rod-plane SF<sub>6</sub> gas gap under double exponential lightning impulse voltage has been investigated by Lu Zhang. It was found that

when wave front time varies in the range of 0.08~1.2μs, 50 % breakdown voltage of the gap declines first and then rise up again to form a curve in the shape of “U” [13]. In addition, Tao Wen studied the influence of wave tail time on the 50 % breakdown voltage and found that the 50 % breakdown voltage of rod-plane SF<sub>6</sub> gas gap decreased as the wave tail time increased. The larger the electric field non-uniform factor, the faster the 50 % breakdown voltage declined with the increase of wave tail time [14]. His study also implied that the degree of electric field non-uniformity would affect the shape of *V-t* characteristics curves. In these studies, rod-plane SF<sub>6</sub> gaps were used to simulate a non-uniform electric field in GIS, but the situation is not identical to the field distribution in GIS with defects, especially when metal particles attach onto the bus or the surface of insulators. Therefore, the applicability of these results still need to be further verified.

In this paper, a test platform was established based on 1 MV Marx generator and coaxial bus of a 220 kV GIS, and a spike defect attached onto the inner conductor surface was provided to simulate a severe non-uniform electric field. 50 % breakdown voltage, as well as *V-t* characteristics under impulse voltages with various wave front times and the same wave tail time were investigated, so as to get further understanding of discharge characteristics in highly non-uniform electric field in GIS, which will be helpful to improve the insulation defects detection in hand-over test.

## 2 EXPERIMENT CONDITIONS

### 2.1 DEFECT MODELS

A stainless steel needle with 1mm in diameter and several μm radius of curvature at the tip was chosen to simulate local electric field concentration caused by spike defect in GIS. Specific electrode structure of paper, which is shown in Figure 1, is more reasonable compared to rod-plane SF<sub>6</sub> gap. The length (*l*) of the needle was set as 3, 5, 7 and 10 mm and the degrees of of the SF<sub>6</sub> gap with different needles were calculated by using Ansoft simulation software. The results were shown in the Table 1. A factor *f* was used to describe the degree of electric field non-uniformity, and according to the length of the needle, the factor ranged from about 30 to 70. Considering the ablation of discharge when SF<sub>6</sub> gap breaks down under impulse, the radius of curvature at needle tip will be gradually coarsen to about 100 μm, so the steel needle was replaced by new ones after every 10 discharges.

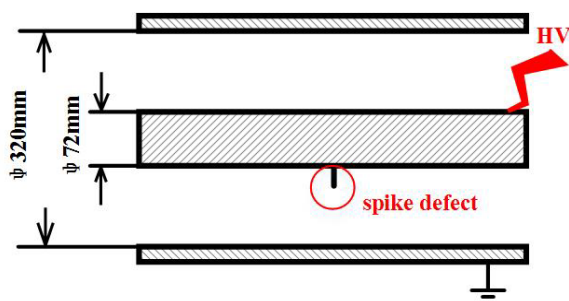


Figure 1. Coaxial bus with a spike defect.

Table 1. Different electric field non-uniformity factors corresponding to different spike defects.

length of spike defect ( <i>l</i> )	electric field non-uniformity factor ( <i>f</i> )
3mm	29.9
5mm	43.3
7mm	55.0
10mm	70.6

### 2.2 EXPERIMENT PLATFORM

The configuration of experimental setup was shown in Figure 2, including control unit, trigger and power supply unit, Marx generator, and a GIS bus. By changing the wave front resistor and steepening gap of Marx generator, five kinds of double exponential impulse voltages can be obtained, as shown in Figure 3. The wave front times were 0.08, 0.40, 0.90, 8.0, and 15.0 μs, respectively, while the wave tail times were the same of 46.5 μs. The stainless steel needle was attached onto the high voltage conductor in the section of experimental chamber.

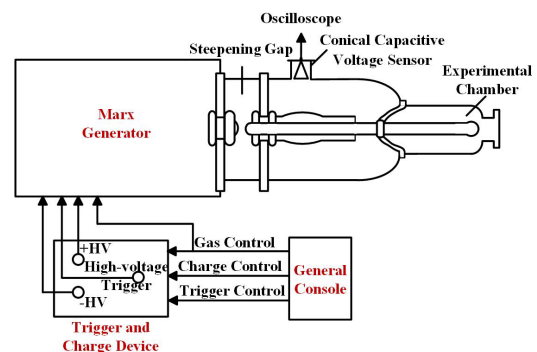
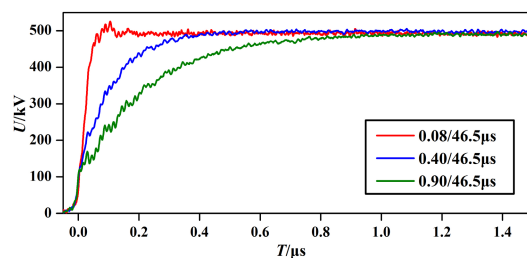
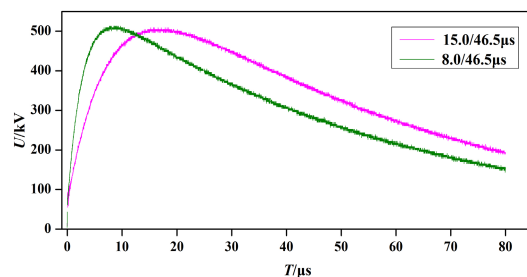


Figure 2. Configuration of experimental setup.



(a) Waveforms with front of 0.08μs, 0.40μs and 0.90μs.



(b) Waveforms with front of 8.0μs and 15.0μs.

Figure 3. Double exponential impulse voltages with different wave front times.

The impulse measuring system consists of a conical capacitive voltage divider, double shielded cable, coaxial integrator and digital oscilloscope. The high-voltage arm of conical capacitive voltage divider is composed of the capacitance formed by the GIS HV bus and the conical voltage divider electrode. A polyimide film (PI) with a few microns thick between the inner and outer aluminum cones is the dielectric of the low-voltage arm capacitance [15]. The average voltage division ratio of this system is 36263 and the measurement uncertainty is less than 2 %. The digital oscilloscope used in the experiment is Tektronix DPO4104, with a bandwidth of 1 GHz and a sampling rate of 5 GHz, which can well meet experimental measurement requirements.

### 2.3 EXPERIMENT METHOD

By adjusting SF<sub>6</sub> pressure in experiment chamber, wave front time of double exponential impulse voltage and length of spike defect, 50% breakdown voltage and  $V-t$  characteristics of SF<sub>6</sub> gas gap have been studied under 5 different impulse voltages. To ensure that data points were effective when up-and-down method was applied to study 50 % breakdown voltages, at least 15 shots were carried out for each data point, and time interval between each shot was about 5 minutes. But in  $V-t$  characteristics test, no less than 50 shots were carried out while time interval between each shot was also about 5 minutes [16].

All of the impulse voltages applied in the experiments were positive, and the effect of voltage polarity on discharge characteristics will not be discussed in this paper.

## 3 RESULTS AND DISCUSSION

### 3.1 INFLUENCE OF GAS PRESSURE ON DISCHARGE CHARACTERISTICS OF SF<sub>6</sub> GAS GAP

Figure 4 presents experiment results of 50 % breakdown voltages with different SF<sub>6</sub> gas pressures ranged from 0.1MPa to 0.6 MPa. Four kinds of impulses with wave front time of 0.08, 0.40, 0.90, and 15.0μs were applied when the length of spike defect was 10 mm.

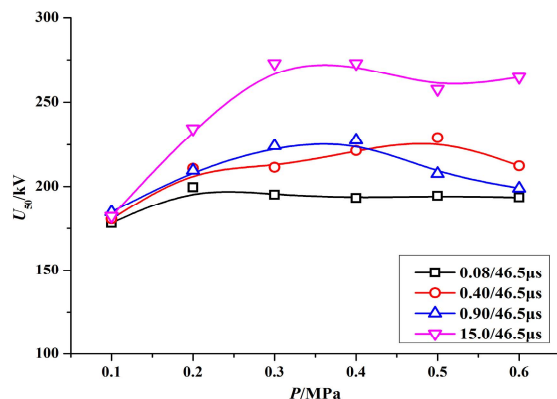


Figure 4. 50% breakdown voltage with different gas pressures.

It is indicated that when wave front time is very short ( $t_f=0.08\mu s$ ), there is no significant variation of 50%

breakdown voltage when gas pressure changes, especially when gas pressure ranges from 0.2 to 0.5 MPa. However, when the wave front time increases to about hundreds of nanoseconds, 50 % breakdown voltage increases first and then decreases as SF<sub>6</sub> pressure increases, so  $U_{50\%}-P$  seems to be hump curves.

When wave front time is rather short, taking  $t_f=0.08\mu s$  as an example, the impulse voltage rises so fast that positive space charges generated by corona discharge hardly transport around, so they gather together in the vicinity of the tip of spike defect. Owing to the high electric field strength around spike defect ( $f=70.6$ ), it is easy to burst a strong ionization process in this region [17], which will accelerate the transformation process of a streamer to a leader and finally cause the initiation of leader discharge. Previous researches concluded that when the voltage of a leader head exceeds a critical value ( $U_{cr}$ ) which only has very weak positive correlation with pressure, the leader could propagate forward [18-20]. Therefore, in Figure 4, the 50 % breakdown voltage does not change with pressure.

Once wave front time increases, rising gradient of impulse voltage turns to be relative lower, so the ionization process is weakened, and the number of space charges increases more slowly. When SF<sub>6</sub> pressure is low, space charges are more likely to spread out, thus electric field distribution around the spike defect will be improved and so called corona stabilization effect can lead to the increase of impulse breakdown voltage.

Positive ions in ionization zone turn to be more difficult to diffuse with the rise of SF<sub>6</sub> gas pressure, so they accumulate around spike defect and intensify the distortion degree of electric field, which will finally cause a reduction of impulse breakdown voltage. It is assumed that when SF<sub>6</sub> pressure is raised to certain value, no corona will occur before breakdown, and the impulse breakdown voltage will rise again as SF<sub>6</sub> pressure continues to be raised. As a result,  $U_{50\%}-P$  curves with longer wave front times seem to be humps, and the corresponding gas pressures at peak points of  $U_{50\%}-P$  curves are different according to various wave front times of impulse voltages.

Figure 5 presents the  $V-t$  characteristics of SF<sub>6</sub> gas gap under two kinds of impulses (0.08/46.5μs and 0.40/46.5μs) with gas pressure ranged from 0.3MPa to 0.6MPa, and the length of spike defect was 10mm. The results indicate that under these two kinds of impulses, the  $V-t$  characteristics are almost the same at various gas pressures. This phenomenon could be explained by streamer-leader step-by-step development mechanism. It is known that discharge delay ( $t_b$ ) can be expressed as:

$$t_b = t_0 + t_s + t_a \quad (1)$$

where,  $t_0$  is the time required for voltage to rise to a steady breakdown voltage ( $U_0$ );  $t_s$  represents statistical time delay;  $t_a$  represents formation time delay [21-22].

For a long gas gap,  $t_b$  mainly depends on  $t_a$ , which is usually determined by discharge process. In a highly inhomogeneous

electric field with high pressure, discharge process can be summarized as: after the formation of the first leader, a new streamer corona will emerge at the head of this leader, and after a certain time delay the streamer corona will transform into leader too. This process repeats constantly and the leader develops forward step by step till the gas gap finally breaks down.

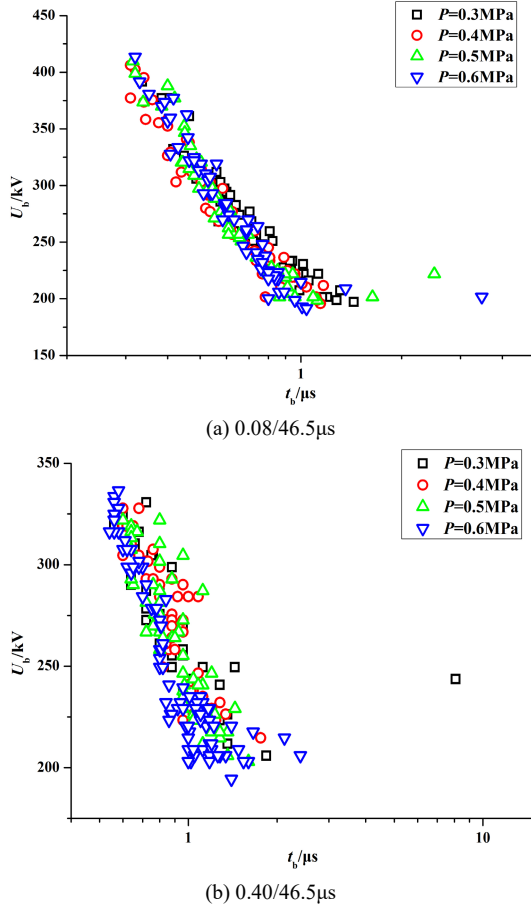


Figure 5.  $V-t$  characteristics with SF<sub>6</sub> gas pressures.

Obviously,  $t_a$  is related with the time interval required for a streamer corona transform into a leader ( $t_L$ ) and the axial length of each streamer corona ( $D_i$ ).  $t_L$  can be calculated by  $t_L=1.68/(PU)$ , where  $P$  represents for pressure and  $U$  represents for voltage [18]. Therefore,  $t_L$  the same as  $D_i$ , decreases with increase of gas pressure [19], which makes the total development time intervals of leaders are almost the same, and  $V-t$  characteristics at different gas pressures almost coincide.

It is worthy to note that a leader is not developing along the axial direction completely, but the development path of a positive streamer is relatively concentrated and gas pressure (0.3MPa ~0.6MPa) is relatively high, so it is assumed that total development lengths of leaders at different pressures were the same.

### 3.2 INFLUENCE OF WAVE FRONT TIME ON DISCHARGE CHARACTERISTICS OF SF<sub>6</sub> GAS GAP

Figure 6 indicates 50 % breakdown voltage rises with the increase of wave front time with different lengths of spike

defect. When the spike is 3 mm, the output voltage of 1 MV generator is not sufficient to get 50 % breakdown voltage under impulse voltage with wave front time of 15  $\mu s$ .

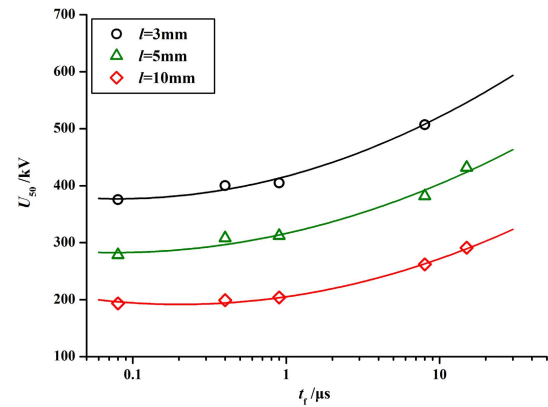
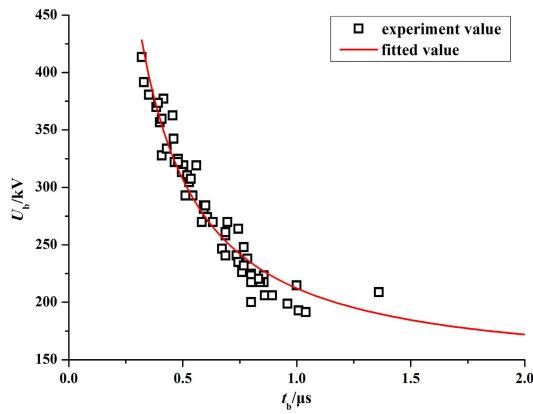


Figure 6. 50 % breakdown voltages with different wave front times.

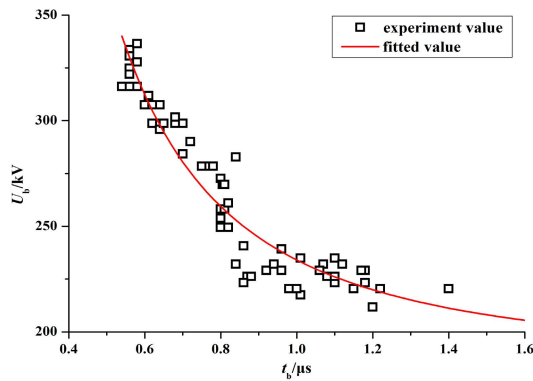
As mentioned in Section 3.1, before impulse voltage rises to steady breakdown value of SF<sub>6</sub> gap, corona discharge occurs at the tip of spike defect and then causes strong ionization. If the length of spike defect and SF<sub>6</sub> pressure were fixed at certain values, while wave front time is short ( $t_f=0.08, 0.40,$  and  $0.90\mu s$ ), space charges in the vicinity of spike defect can hardly move around, so they strengthen the electric field nearby the tip of spike defect, and then aggravate initiation process of a streamer as well as transformation of streamer to leader. Therefore, 50 % breakdown voltages under relative steeper wave front times are lower, and there is no remarkable difference in 50 % breakdown voltages with wave front time of 0.08, 0.40, and  $0.90\mu s$ . On the contrary, when impulse wave front time is 9  $\mu s$ , or even longer, the space charges generated by corona discharge and ionization are more likely to migrate to larger region and weaken the electric field around the spike defect. That means in this situation, the initiation of a streamer is difficult, which leads to the increase of 50 % breakdown voltage under impulse voltage.

In Figure7, significant differences exist in  $V-t$  characteristics with different waveforms. When wave front time of impulse voltage is relatively short, discharge time decreases with the increase of breakdown voltage. On the contrary, discharge time increases with the increase of breakdown voltage when wave front time is longer than several microseconds.

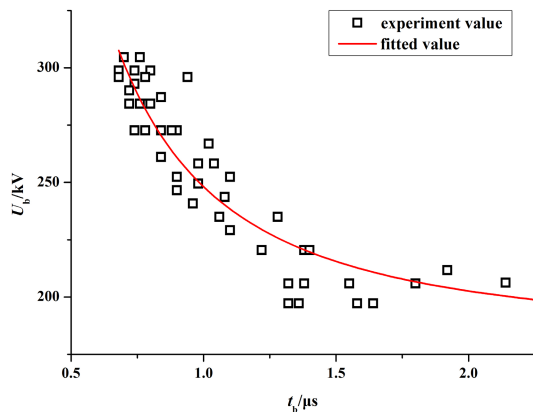
In the former situation, gap often breaks down at wave tail and data points in the graph of  $V-t$  curves represent peak values. So when breakdown voltage rises, it means peak value of impulse, as well as voltage rising rate ( $dU/dt$ ) will increase accordingly, which may cause the increase of probability for a free electron to transform into an effective initial electron in SF<sub>6</sub> gas gap, and finally lead to a decrease of average statistical time delay ( $t_s$ ). Furthermore, the time interval required for a streamer corona to transform into a leader,  $t_L=1.68/(PU)$  can also be reduced with the rise of breakdown voltage. As a result, total discharge time delay,  $t_b = t_0 + t_s + t_a$



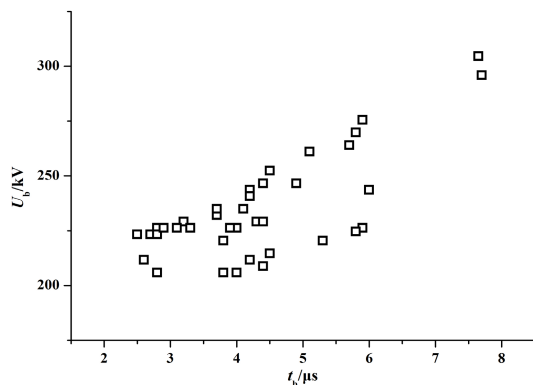
(a) 0.08/46.5 μs



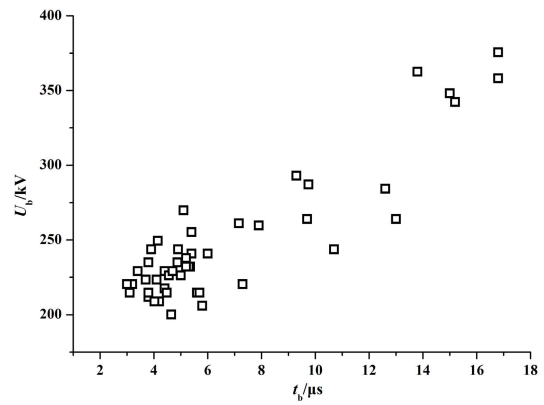
(b) 0.40/46.5 μs



(c) 0.90/46.5 μs



(d) 8.0/46.5 μs



(e) 15.0/46.5 μs

Figure 7.  $V-t$  characteristics with different waveforms.

decreases. But in the latter situation,  $dU/dt$  turns to be lower and impulse voltage duration becomes longer, expanded space charge layer improves the electric field distribution nearby the spike defect, thus increases breakdown voltage [23].

Therefore, an empirical formula for engineering application is used to fit the  $V-t$  characteristics of the first three waveforms [24-26]. Results are shown as the solid lines in Figure 7a-c. The Equation can be expressed as:

$$U_b(t) = U_{bmin} + \frac{aU_{bmin}}{t^n} \quad (2)$$

In Equation (2),  $U_{bmin}/kV$  represents for the minimum breakdown voltage under impulse voltage. It is assumed that breakdown voltage of  $SF_6$  gas gap obeys normal distribution  $N(U_{50}, \sigma)$ , so  $U_{bmin} = U_{50} - 3\sigma$ .  $a$  represents the rising rate of breakdown voltage at  $t=1\mu s$ .  $t/\mu s$  represents breakdown time delay and  $n$  is a constant which decides the descent speed of breakdown voltage with the increase of breakdown time delay.

However, when wave front time becomes longer, slope of  $V-t$  characteristics curve is positive and it cannot be fitted by Equation (2). Considering that the voltage rising rate ( $dU/dt$ ) has great influence on discharge process under this circumstance, the relationship between average voltage rising rate and  $t_b$  is analyzed. The results with  $t_f=8.0\mu s$  are shown in Figure 8a, it can be fitted by Equation (3) shown as below:

$$\overline{\left(\frac{dU_b}{dt}\right)} = 20 + \frac{118.64}{t_b - 0.78} \quad (3)$$

Further, it can be derived to get the relationship between  $U_b$  and  $t_b$ :

$$U_b = 20t_b + \frac{118.64t_b}{t_b - 0.78} \quad (4)$$

The  $V-t$  curve with  $t_f=8.0\mu s$  can be also fitted by using Equation (4), and the result is shown in Figure 8b.

Similarly, the relationship between average voltage rising rate and  $t_b$  at  $t_f=15.0\mu s$  is shown in Figure 9a. It can be fitted by Equation (5):

$$\overline{\left(\frac{dU_b}{dt}\right)} = 11.32 + \frac{155.24}{t_b - 0.51} \quad (5)$$

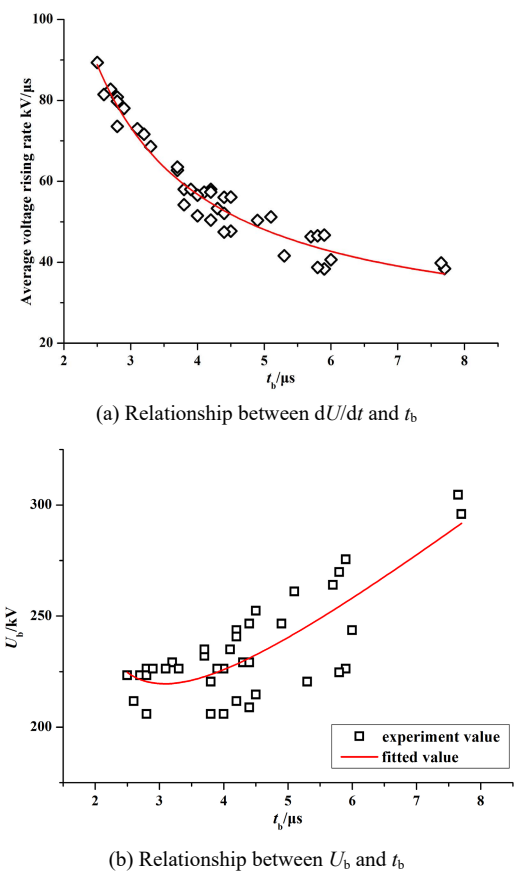


Figure 8.  $V-t$  characteristics under the impulse voltage of 8.0/46.5  $\mu$ s.

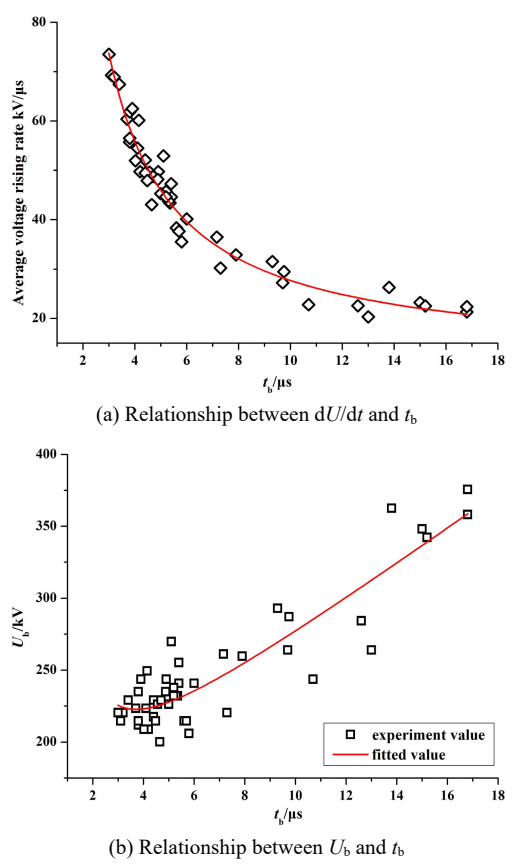


Figure 9.  $V-t$  characteristics under the impulse voltage of 15.0/46.5  $\mu$ s.

And it can also be derived to get the relationship between  $U_b$  and  $t_b$  when  $t_f$  is 15.0  $\mu$ s:

$$U_b = 11.32t_b + \frac{155.24t_b}{t_b - 0.51} \quad (6)$$

The  $V-t$  curve when  $t_f$  is 15.0  $\mu$ s can be fitted by using Equation (6), and the result is shown in Figure 9b. It can be seen from these figures that this method is better for fitting  $V-t$  characteristics curves under impulse voltage with wave front time in the range of several microseconds to several tens of microseconds.

### 3.3 INFLUENCE OF ELECTRIC FIELD NON-UNIFORMITY ON DISCHARGE CHARACTERISTICS OF SF<sub>6</sub> GAS GAP

It is shown in Figure 10 that 50% breakdown voltage almost decreases linearly with the increase of electric field non-uniformity factors ( $f$ ) when SF<sub>6</sub> pressure is 0.6 MPa. As  $f$  rises, electric field near the spike defect is seriously distorted, corona discharge will occur at relative lower voltage. Then, large amount of electrons are generated and lead to the initiation of streamer, which can be easily transformed into leader, and finally cause the decrease of 50 % breakdown voltage.

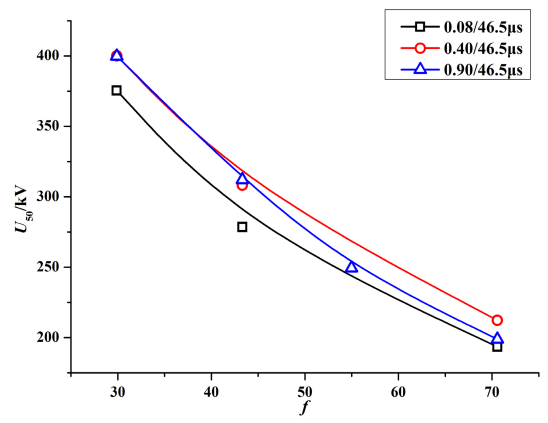


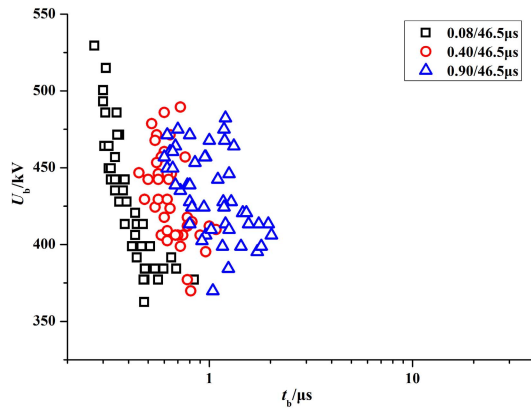
Figure 10. 50 % breakdown voltage with different electric field non-uniformity factors.

Data of  $V-t$  characteristics under different impulse voltages are overlaid into a graph, and the results are shown in Figure 11. When  $f$  increases, the dispersion of the  $V-t$  characteristics cluster is reduced. The initiation of an effective electron in SF<sub>6</sub> gas gap becomes easier when the electric field non-uniformity factors increases, so the dispersion of average statistical time delay ( $t_s$ ) reduces. Therefore, data points in Figure 11 are more intensive when  $f$  is higher (in Figure 11c), and data points are scattered when  $f$  is relatively lower (in Figure 11a and b).

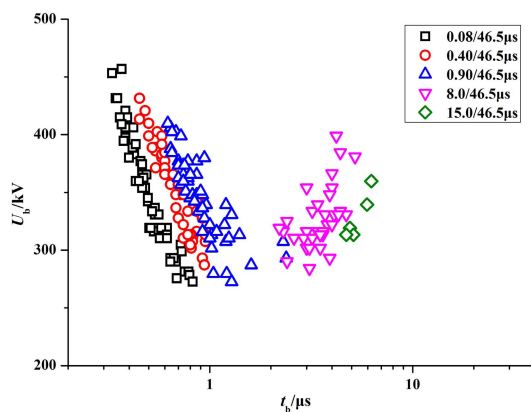
In addition, in Figure 11b and c, the profile of  $V-t$  characteristics seems to be a valley, and the flat part at the bottom of the valley expands with the increase of  $f$ . Under impulse voltages with shorter wave front time, expansion of flat region means the probability of breakdown with long time delay increases, due to more obvious corona stabilization

effect of space charges. But for impulse voltage with longer wave front time, expansion of flat region indicates that more breakdowns occur with a short time delay due to seriously distorted electric field caused by accumulated space charges nearby the spike defect in the rising stage of impulse voltage.

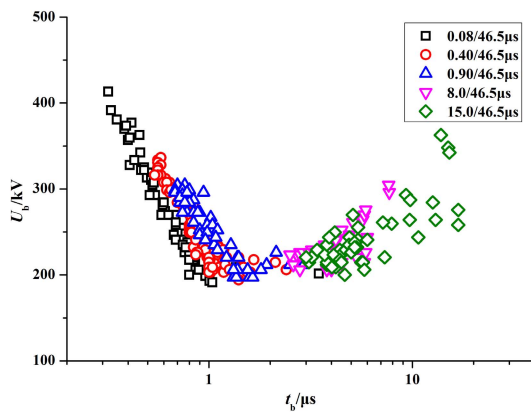
The minimum breakdown voltage under different  $f$  can be obtained by the above-mentioned valley profile. It is of certain engineering significance to guide the design of GIS insulation.



(a)  $f=29.9$



(b)  $f=43.3$



(c)  $f=70.6$

Figure 11. Laws of voltage-time characteristics changing with electric field non-uniform factor.

## 4 CONCLUSION

By using 1MV Marx generator and coaxial GIS bus, breakdown experiments under five kinds of double exponential impulse voltages are applied to GIS bus with a spike defect on the high voltage conductor. Following conclusions are obtained:

- 1) When wave front time is very short, 50 % breakdown voltage of SF<sub>6</sub> gas gap hardly changes with pressure. As wave front time increasing,  $U_{50\%}-P$  curve gradually turns to be a hump. However, pressure has no effect on  $V-t$  characteristics under the conditions mentioned in this paper.
- 2) When wave front time of double exponential impulse voltage increases, 50 % breakdown voltage of SF<sub>6</sub> gas gap increases. The slope of  $V-t$  characteristics curve is negative when wave front time of impulse voltage is relative short, and the slope turns to be positive when wave front time is increased to several microseconds.
- 3) A new method is proposed to fit  $V-t$  characteristics curves under impulse voltage with wave front time of several microsecond, since voltage rising rate ( $dU/dt$ ) has great influence on the discharge process in this situation. The fitting results are proved to be satisfying.
- 4) With the increase of electric field non-uniformity factors ( $f$ ), 50 % breakdown voltage of SF<sub>6</sub> gas gap decreases almost linearly.  $V-t$  characteristics curves with profile of valley at different  $f$  are drawn. When  $f$  increases, the dispersion of  $V-t$  characteristics cluster is reduced but flat region of the valley-like curve expands.

## ACKNOWLEDGMENT

This work was financially supported by the National Key R&D Program of China (2017YFB0903800).

## REFERENCES

- [1] A. Sabot, A. Petit, and J. Taillebois, "GIS insulation co-ordination: Onsite tests and dielectric diagnostic techniques, A utility point of view," IEEE Trans. Power Del., vol. 11, pp. 1309–1316, 1996.
- [2] J. Kang, S. Xu, J. Li, B. He, K. Meng, T. Wu, Z. Zhang, Y. Wang, L. Ma, Y. He, and P. Liao, "Technical research for field impact test of 800kV GIS equipment," Qin Hai Electr. Power, vol. 30, pp. 1–2, 2011.
- [3] U. Riechert and W. Holaus, "Ultra high-voltage gas-insulated switchgear-A technology milestone," Eur. Trans. Electr. Power, vol. 22, pp. 60–82, 2012.
- [4] L. Li, Y. Shang, L. Zhang, R. Shi, and W. Shi, "Analysis of very fast transient overvoltages (VFTO) from onsite measurements on 800 kV GIS," IEEE Trans. Dielectr. Electr. Insul., vol. 19, pp. 2102–2110, 2012.
- [5] H. Okubo and A. Beroual, "Recent trend and future perspectives in electrical insulation techniques in relation to sulfur hexafluoride (SF<sub>6</sub>) substitutes for high voltage electric power equipment," IEEE Electr. Insul. Mag., vol. 27, pp. 34–42, 2011.
- [6] Q. Zhang, Y. Qiu and P. Wang, "Dielectric characteristics of SF<sub>6</sub> under the steep-fronted impulses," in IEEE International Symposium on Electrical Insulation Proceedings, 1996, pp. 770–773.
- [7] High Voltage Switchgear and Controlgear—Gas-Insulated Metal Enclosed Switchgear, IEC Standard 62271-203, 2003-11.
- [8] High-Voltage Test Techniques—Part 1: General Definitions and Test Requirements, IEC Standard 60060-1, 2010-09.

- [9] S. Okabe, T. Tsuboi, and G. Ueta, "Study on lightning impulse test waveform for UHV-class electric power equipment," IEEE Trans. Dielectr. Electr. Insul., vol. 19, pp. 803–811, 2012.
- [10] S. Okabe, S. Yuasa and S. Kaneko, "Evaluation of Breakdown Characteristics of Gas Insulated Switchgears for Non-Standard Lightning Impulse Waveforms - Breakdown Characteristics for Non-Standard Lightning Impulse Waveforms Associated with Lightning Surges," IEEE Trans. Dielectr. Electr. Insul., vol. 15, pp. 407–415, 2008.
- [11] J. Dupuy and A. Gibert, "Comparison of Point-Plane Discharge in Air and SF<sub>6</sub>," J. Phys. D: Appl. Phys., vol. 15, pp. 655–664, 1982.
- [12] Z. Guo, X. Zhao and C. Gu. "Discharge Characteristics of SF<sub>6</sub> Non-uniform Field Gap under Oscillating Impulses," High. Vol. Appa., vol. 46, pp. 62–64, 2010.
- [13] L. Zhang, Q. Zhang and Y. Yin. "Voltage-time Characteristics of Long SF<sub>6</sub> Gap under VFTO and Lightning Impulse," High Vol. Engineer., vol. 39, pp. 1396–1401, 2013.
- [14] T. Wen, Q. Zhang and J. Ma. "Discussion on Lightning Impulse Test Waveform According to Breakdown Characteristics of SF<sub>6</sub> Gas Gaps," IEEE Trans. Dielectr. Electr. Insul., vol. 24, pp. 2306–2313, 2017.
- [15] T. Wen, Q. Zhang and C. Guo. "3-MV compact very fast transient overvoltage generator for testing ultra-high-voltage gas-insulated switchgear," IEEE Electr. Insul. Mag., vol. 30, pp. 26–33, 2014.
- [16] M. Koch, U. Straumann and C. M. Franck, "Determination of waiting times between successive breakdown experiments," in *Annual Report on IEEE Conference on Electrical Insulation and Dielectric Phenomena*, 2012, pp.349–352.
- [17] G. Ueta, S. Kaneko, and S. Okabe, "Evaluation of breakdown characteristics of gas insulated switchgears for non-standard lightning impulse waveforms—Breakdown characteristics under non-uniform electric field," IEEE Trans. Dielectr. Electr. Insul., vol. 15, pp. 1430–1438, 2008.
- [18] K. Tekletsadik and L. Campbell, "SF<sub>6</sub> breakdown in GIS," in Proc. IEEE Sci., Meas. Technol., vol. 143, pp. 270–276, 1996.
- [19] L. Niemeyer, L. Ullrich and N. Wiegart, "The mechanism of leader breakdown in electronegative gases," IEEE Trans. Electr. Insul., vol. 24, pp.309–324, 1989.
- [20] F. Pinnekamp and L. Niemeyer, "Qualitative model of breakdown in SF<sub>6</sub> in inhomogeneous gaps," J. Phys. D: Appl. Phys., vol. 16, pp. 1293, 1983.
- [21] J. Laghari and A. Qureshi, "A review of particle-contaminated gas breakdown," IEEE Trans. Dielectr. Electr. Insul., vol. 16, pp. 388–398, 1981.
- [22] Z. Milanović, K. Stanković and M. Vujisić, "Calculation of impulse characteristics for gas-insulated systems with homogenous electric field," IEEE Trans. Dielectr. Electr. Insul., vol. 19, pp. 648–659, 2012.
- [23] T. Hibma and H. R. Zeller, "Direct Measurement of Space-Charge Injection from a Needle Electrode into Dielectrics," J. Appl. Phys., vol. 59, pp.1614–1620, 1986.
- [24] A. Ancajima, A. Carrus and E.Cinieri. "Optimal selection of disruptive effect models parameters for the reproduction of MV insulators volt-time characteristics under standard and non-standard lightning impulses," IEEE Power Tech, pp. 760–765, 2008, Lausanne.
- [25] B. Sharath and S. Usa. "Prediction of impulse voltage-time characteristics of air and oil insulation for different wavefronts," IEEE Trans. Dielectr. Electr. Insul., vol.16, pp. 1693–1697, 2009.
- [26] G. Krithika and S. Usa. "V-t Characteristics using extended disruptive effect model for impulses of varying front times," IEEE Trans. Dielectr. Electr. Insul., vol. 22, pp. 2191–2195, 2015.



**Xuandong Liu** was born in Sichuan, China, in 1981. He received the B.S. degree in automation from the Chongqing University of Post and Telecommunication, Chongqing, China, in 2004, and the Ph.D. degree from Xi'an Jiaotong University, Xi'an, China, in 2011. He is currently an Associate Professor with the State Key Laboratory of Electrical Insulation and Power Equipment, Xi'an Jiaotong University.



**Lingli Zhang** was born in Jiangsu, China in 1992. She received the B.S. degree from Xi'an Jiaotong University, Shaanxi, China in 2015. She is currently a postgraduate student at the High Voltage Division, School of Electrical Engineering, and the State Key Laboratory of Electrical Insulation and Power Equipment. She is now engaged in the research of GIS insulation features.



**Tao Wen** was born in Shaanxi, China, in 1990. He received the BS degree in electrical engineering from Xi'an Jiaotong University, Xi'an, China, in 2012. He is currently working toward a PhD degree at the High Voltage Division, School of Electrical Engineering, and the State Key Laboratory of Electrical Insulation and Power Equipment, Xi'an Jiaotong University. Beginning in 2016, he has been working toward a doctoral double degree program at Tokushima University, Tokushima, Japan.



**Qiaogen Zhang** received the B.S., M.S., and Ph.D. degrees in electrical engineering from Xi'an Jiaotong University, Xi'an, China, in 1988, 1991, and 1996, respectively. He is currently a Professor with the High Voltage Division, School of Electrical Engineering, and the State Key Laboratory of Electrical Insulation and Power Equipment, Xi'an Jiaotong University. His major research interests include outdoor insulation, pulse power technology, gas discharge and its application.